Study of Ion Cyclotron Emissions due to DD Fusion Product Ions on JT-60U

M. Ichimura 1), M. Katano 1), Y. Yamaguchi 1), S. Sato 1), Y. Motegi 1), H. Muro 1), T. Ouchi 1), S. Moriyama 2), M. Ishikawa 2), K. Shinohara 2), Y. Sakamoto 2), A. Kojima 2), T. Watanabe 3)

1) Plasma Research Center, University of Tsukuba, Tsukuba, Ibaraki 305-8577, Japan
2) Japan Atomic Energy Agency, Naka, Ibaraki 311-0193, Japan
3) National Institute for Fusion Science, Toki 509-5292, Japan

e-mail contact of main author: ichimura@prc.tsukuba.ac.jp

Abstract. In this paper, ion cyclotron emissions (ICEs) due to deuterium-deuterium (DD) fusion-product (FP) ^{3}He, T and P-ions on JT-60U are described. Electromagnetic waves with finite toroidal wave numbers are detected by using ion cyclotron range of frequency antennas as pickup loops. The toroidal wave numbers are evaluated from the phase differences between two antenna straps arrayed in the toroidal direction. The excitation of the fast Alfvén waves for the mechanism of ICEs due to ^{3}He and P-ions, ICE(^{3}He) and ICE(P), is consistent with that in the previous JET and TFTR experiments. ICE due to T-ions, ICE(T), with lower frequency has larger wave numbers than ICE(^{3}He). The excitation of the slow Alfvén waves is elucidated for the first time as the mechanism for ICE(T). The density dependence for the excitation of the fundamental and the second harmonic ICEs(^{3}He) is obtained. The fundamental ICE(^{3}He) appears only in relatively low density operation. A frequency peak due to FP-ions sometimes splits into a doublet shape as observed in JET experiments. The phase differences of both peaks are detected to be positive and negative values and indicate that two waves are traveling in both toroidal directions. The anisotropy of the FP T-ions at the outer plasma edge is evaluated by using 'Escape Particle Orbit analysis Code (EPOC)'. The precise behaviors of ICEs due to FP-ions on JT-60U are studied.

1. Introduction

In high-beta plasma experiments, fluctuations in the ion cyclotron range of frequency (ICRF) have been observed due to the anisotropy of energy distribution and the presence of non-thermal ion components. The Alfvén-ion-cyclotron (AIC) mode is one of the typical micro-instabilities excited in the mirror plasmas with the strong temperature anisotropy [1-3]. On the other hand, ion cyclotron emissions (ICEs), of which frequencies are the ion cyclotron frequency and its higher harmonics for the magnetic field strength of the outermost magnetic surface at the outer plasma edge, have been reported in a decade from 1990 on JET, TFTR and JT-60U [4-8]. The high-energy fusion-product (FP) ions are trapped in the local mirror configuration and undergo large excursion orbits from the plasma center to the plasma edge. Such high-energy FP-ions form the non-thermal ion distribution near the plasma edge. The excitation of the fast Alfvén waves is considered to be the most probable origin of ICEs due to FP-ions [5]. Recently, on the neutral-beam (NB) injection heated deuterium (D) plasmas in JT-60U, ICEs due to injected D-ions and FP ^{3}He and T-ions have been analyzed by using ICRF antennas as pickup loops [9].

In JT-60U, the spatial structures of excited waves can be measured by using ICRF antenna straps arrayed in poloidal and toroidal directions. From the measurement in the poloidal direction, both ICEs due to injected D-ions, ICEs(D) and FP-ions have been confirmed to be electromagnetic fluctuations. From the measurement in the toroidal direction, it becomes clear that ICEs(D) have no toroidal wave numbers and ICEs due to FP-ions have finite wave numbers. The behaviors of ICE due to ^{3}He-ions, ICE(^{3}He), are consistent with those in the previous JET and TFTR experiments. However, ICE due to T-ions, ICE(T), of which frequency is much lower than the cyclotron frequency of the outermost magnetic surface at the outer plasma edge, is observed when negative-ion based neutral beams (N-NB), of which energy is more than $300 keV$, are injected tangentially. To study spontaneously excited waves in ICRF and the basic physics in the magnetically confined plasmas with non-thermal energy distribution is the main motivation of this work. Recently, ICE due to FP P-ions is also observed. To use ICEs as a significant diagnostic tool for fusion reactions, it is necessary to understand the precise mechanism of the wave excitation.

2. Experimental setup

Conventional positive-ion based neutral beams (P-NBs, injection both in perpendicular and tangential directions), of which energy is around $80keV$, and N-NBs, of which energy is around $300keV$, are normally used for the high performance D-plasma operation on JT-60U [10]. Deuterium-deuterium (DD) fusion neutrons are detected and confirm the realization of DD fusion reactions and production of DD FP-^{3}He, T and P-ions. Two ICRF antennas installed on the outer midplane of the vacuum vessel are used as pickup loops for detecting electrostatic and/or electromagnetic fluctuations. Two straps (separated with $0.44m$ in the toroidal direction) are arrayed in each ICRF antenna. Straps are grounded at the center and both ends of each strap are connected to the output of rf generators through the vacuum feed-through, the matching components and the transmission lines. Then, four loops in two columns and two rows are set for each ICRF antenna as shown in Fig.1. The width of each strap is $0.19m$. Single layer Faraday shield is used and a good coupling for the rf field is expected electro-statically and/or electro-magnetically. The current in both loops on each strap induced by the time derivative of the magnetic field component has the opposite sign because of their opposite loop direction. On the other hand, electric potentials are detected when the plasma and antenna couples electro-statically. The voltage signals on both loops due to the electric field component have the same sign as indicated in the figure. Two sets of ICRF antennas, which are installed with the distance of $1.67m$ in the toroidal direction, are used in this experiment and the toroidal wave number can be evaluated due to the small pitch angle of the toroidal magnetic field line.

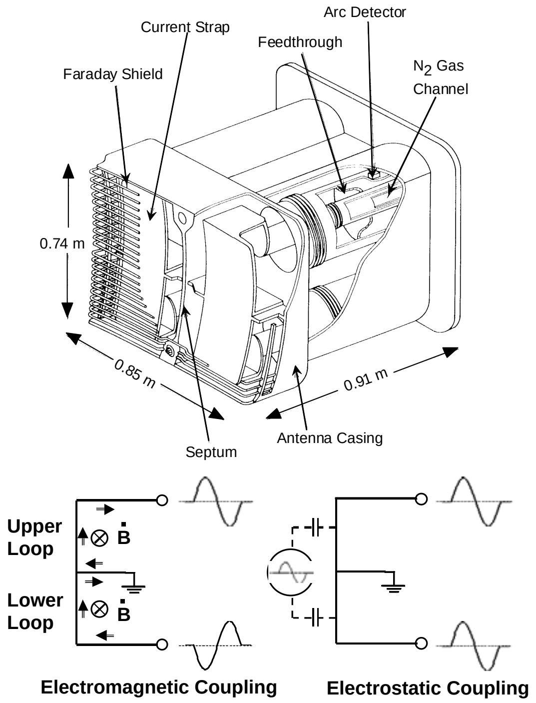

FIG.1 Schematic drawing of ICRF antenna: four current loops are arrayed in two columns and two rows. Schematic drawing of loops for electromagnetic and electrostatic coupling schemes is indicated including the flow direction of induced current for the electromagnetic coupling and induced voltage for the electrostatic coupling.

Signal cables are connected directly to the transmission line between the antenna strap and the matching components outside of the vacuum feed-through. The matching components are disconnected. Detected signals are transmitted to the data acquisition system located in JT-60U control room. To determine the phase differences between two loops correctly, the signal cables with a total length of more than $400m$ are used and their effective electrical lengths including coaxial lines, coaxial cables are calibrated precisely by measuring the propagation time of the incident and reflected electric pulses. Signals are recorded by using an oscilloscope with a maximum sampling rate of $500 Ms/s$ (Mega-sampling per second) and a maximum memory length of $12 MW/ch$ (Mega-word per channel). Typically, signals are sampled during $100\mu s$ in every $50ms$ and the temporal behavior of the fluctuations can be analyzed in the duration of more than $10s$ by using a discrete sampling method. When we determine wave numbers, we use three antenna straps and measure the phase differences between every two loops at the same time.

3. Observations of ICEs due to ^{3}He and T-ions

By using ICRF antennas as pickup loops, the electromagnetic flucturations have been clearly detected and their toroidal structures have been evaluated from the phase differences between two antenna straps arrayed in the toroidal direction. Figure 2(c) shows a typical intensity plot of the temporal evolution of the frequency spectrum in the case of the tangential P-NBs, perpendicular P-NBs and N-NBs injections, on which both of ICE(^{3}He) and ICE(T) are detected at the same time. The temporal evolution of (a) NB powers and (b) plasma parameters (line averaged density and diamagnetic signal) are indicated in the figure. The temporal evolution of the amplitude of each ICE and the signal of fusion neutrons are also indicated in Fig.2(d). Two sharp peaks, of which frequencies are corresponding to the 2nd harmonic cyclotron frequency of ^{3}He-ions and a fundamental cyclotron frequency of T-ions near the outer plasma edge, are clearly observed. The relatively broad peaks are ICEs due to injected D-ions. The amplitude of the second harmonic ICE(^{3}He) becomes weak when the density and the signal of fusion neutrons start to increase and becomes strong again at the end of the discharge. The amplitude of ICE(T) is almost proportional to the signal of fusion neutrons. As shown in Fig.2(a), several break-downs occur on N-NB and the signal of fusion neutrons follows the N-NB power and also ICE(T) has quick response to the N-NB power.

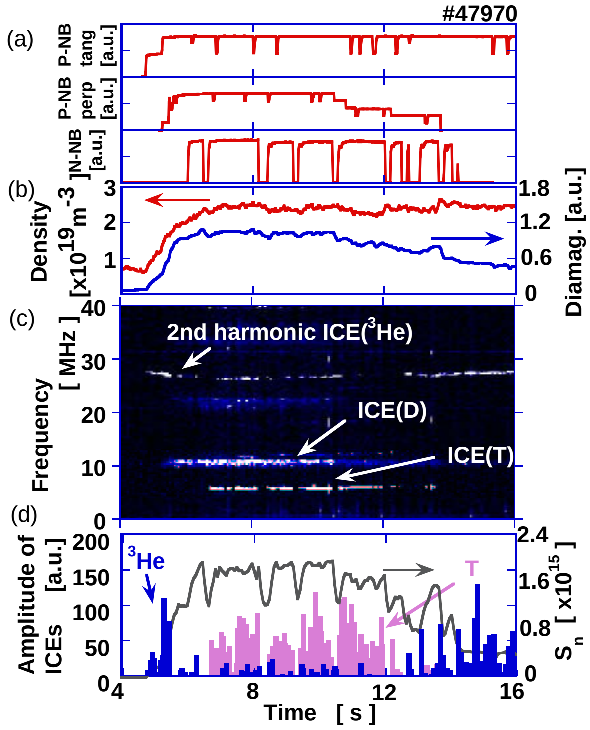

FIG.2 A discharge in which both the second harmonic ICE(^{3}He) and ICE(T) are detected at the same time. Temporal evolution of (a) NB powers, (b) line averaged density and diamagnetism, (c) frequency spectrum of excited waves, (d) amplitude of excited waves and neutron signal is indicated.

The wave numbers of both excited waves are determined from the measurement of phase differences among three different antenna straps in the same discharge and those of the second harmonic ICE(^{3}He) and the fundamental ICE(T) in this discharge are determined to be around 4 and $8m^{-1}$, respectively.

In the reference 9, the behaviors of ICEs related to NB injections on JT-60U are summarized as followings: ICEs(^{3}He) are observed only when the tangential P-NBs are injected. The amplitude of ICEs(^{3}He) becomes weak or ICEs(^{3}He) disappear when the density increases. The frequencies of ICEs(^{3}He) change slightly with time corresponding to change of the location of the outermost magnetic surface at the plasma edge. ICE(T) is observed only when the tangential N-NBs are injected.

On the discharge of Fig.2, the second harmonic ICE(^{3}He) is observed almost in the whole duration and the fundamental ICE(^{3}He) is not observed. The appearance of the fundamental ICEs(^{3}He) depends strongly on the density. Figure 3 shows the density dependence of the amplitude of ICEs(^{3}He). The fundamental ICE(^{3}He) is observed only in the case of the line-averaged density below $1.3\times10^{19} m^{-3}$ (open circles). The second harmonic ICE(^{3}He) is observed in the higher density region (closed circles). The density dependence of ICEs(^{3}He) will be discussed in the next section.

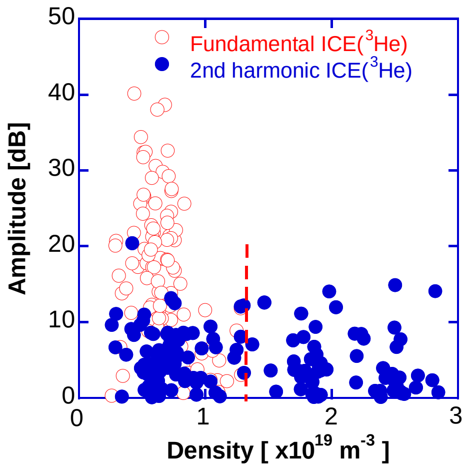

FIG.3 Density dependence of the amplitude of fundamental and second harmonic ICEs(^{3}He). The fundamental ICE(^{3}He)is only observed in low density plasmas.

Recently, ICE due to P-ions, ICE(P), is identified in relatively high density plasmas as shown in Fig.4. In the discharge, the magnetic field strength at the outermost magnetic surface of the outer plasma edge is $1.82T$ and the fundamental cyclotron frequency of D-ions is $13.9MHz$. The second harmonic ICE(D) is detected as the broad frequency peak near $28MHz$. Higher harmonic ICEs(D) are sometimes observed as such broad frequency peaks. A relatively sharp peak is observed just below the second harmonic ICE(D). ICEs due to FP-ions are always excited with the sharp frequency peaks in comparison with ICEs(D). The observed frequencies of ICE(D) are just on the cyclotron frequency and higher harmonic frequencies at the plasma edge. On the other hand, the frequencies of ICEs due to FP-ions are always detected as lower frequencies at the plasma edge as mentioned in reference 11. Most obvious difference between ICEs(D) and ICEs due to FP-ion is the wave number in the toroidal direction [9]. ICEs due to FP-ions have finite wave numbers and can propagate in the toroidal direction. It is confirmed the sharp peak just below the second harmonic ICE(D) has a finite wave number in the toroidal direction and is identified as ICE(P). In the figure, the second

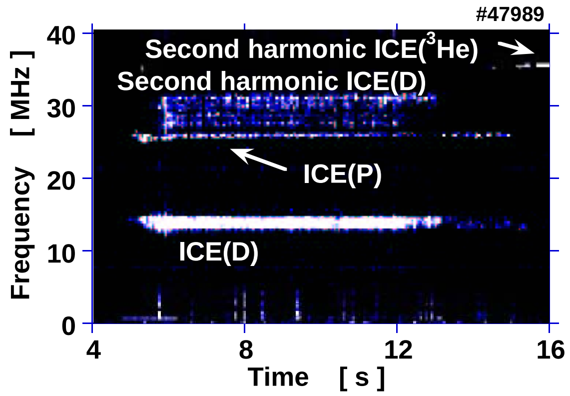

FIG.4 The intensity plot of the temporal evolution of the frequency spectrum in which ICE(P) is clearly observed. From 13 s of the discharge, the density decreases and the second harmonic ICE(^{3}He) appears.

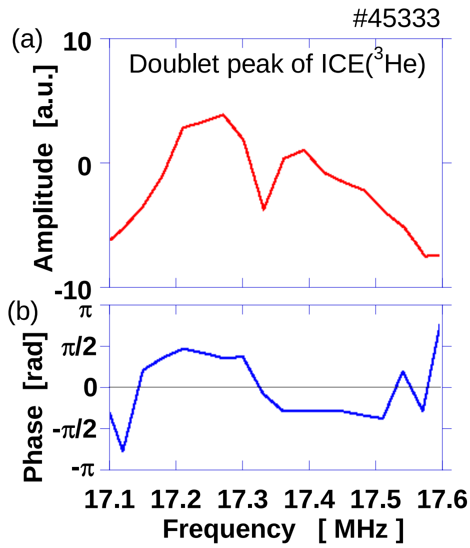

FIG.5 (a) Frequency spectrum of the doublet peak of the fundamental ICE(^{3}He) and (b) the phase difference between antenna straps arrayed in the toroidal direction. Both positive and negative values are clearly measured.

harmonic ICE(^{3}He) is also observed from $15s$, where the density becomes lower than the former duration from $5s$ to $13s$.

It has been reported in JET burning plasma experiments [7] that frequencies of ICEs due to FP-ions are sometimes split into a doublet shape. In JT-60U, the split of the frequency is also observed as shown in Fig.5. The magnetic field strength at the outer plasma edge is $1.8T$ and the cyclotron frequency of ^{3}He-ions is $18.3MHz$ in this discharge. Observed frequency peaks of slightly lower than the cyclotron frequency are corresponding to the fundamental ICE(^{3}He). Figure 5(b) shows the phase differences of the doublet peak between two antenna straps arrayed in the toroidal direction. Both positive and negative phases indicated the propagation to the opposite direction are clearly detected and two waves are traveling in both toroidal directions with the wave numbers of $k_{//} = \pm 2.1$.

4. Interpretation of FP-ICEs on JT-60U

4.1 Dispersion Relation

In the previous section, experimental observations related to ICEs on JT-60U are presented. In this section, the characteristics and interpretation of FP-ICEs in DD fusion plasmas on JT-60U are discussed. In the previous manuscript [9], the obvious difference between ICEs due to FP-ions and ICEs(D) is described to be that of the toroidal wave numbers. The excitation of obliquely propagating fast Alfvén waves (magneto-acoustic waves) is the possible mechanism for ICE(^{3}He) [5]. The dispersion relation of the fast Alfvén waves in D-plasmas with minority ^{3}He-ions is shown in Fig.6(a). Here, the simple dispersion relation of two ion components with Maxwellian distributions is only solved. The realistic dispersion relation including the distribution of energetic FP-ions and quantitative evaluations for the experimental observations are under investigation. Branches of ion-Bernstein waves due to ^{3}He-ions intersect with a branch of fast Alfvén wave in D-plasma. When the density increases, the fast Alfvén wave cannot propagate in the toroidal direction in the low frequency region due to large perpendicular wave numbers and has no intersections with the fundamental branch of ion-Bernstein wave due to ^{3}He-ions as predicted in the figure. The density dependence shown

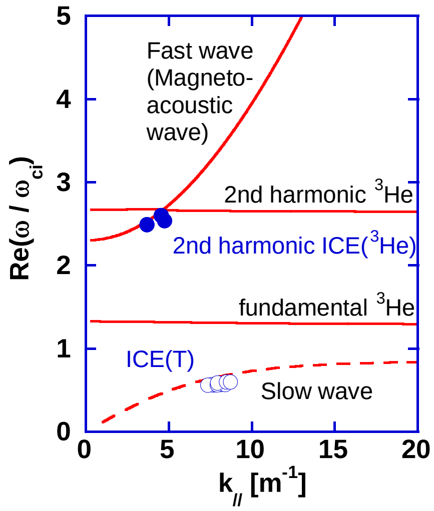

FIG.6(a) Schematic dispersion relation in D-plasmas with minority ^{3}He-ions. Ion Bernstein waves due to minority ions intersect with the fast Alfvén wave. Experimentally observed values are plotted in the figure.

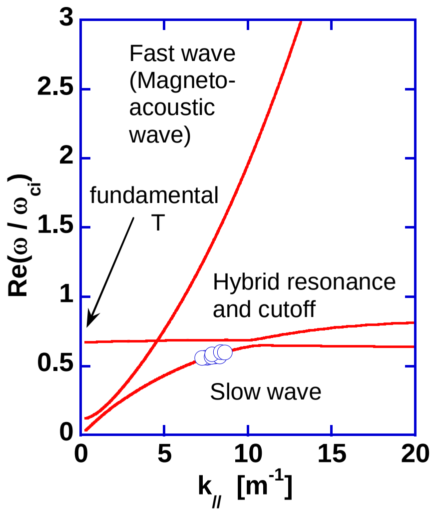

FIG.6(b) Schematic dispersion relation in D-plasmas with minority T-ions. A new cutoff and hybrid resonance appears near the cyclotron frequency of T-ions in Fig.3 will be interpreted as the cutoff property for the wave excitation in the bulk D-plasma.

As measured in the same discharge shown in Fig.2, the toroidal wave number of ICE(T) is larger than that of the second harmonic ICE(^{3}He). This experimental fact indicates ICE(T) is no longer on the same branch of the fast Alfvén wave and ICE(T) may be on the branch of slow Alfvén wave as indicated in Fig.6(a). The dispersion relation of the slow Alfvén waves in D-plasmas with minority T-ions is shown in Fig.6(b). A new cut-off and a new hybrid resonance appear near the cyclotron frequency of T-ions. As also pointed out in the previous report [9], the frequency of ICE(T) is much lower than the cyclotron frequency of T-ions near the outermost magnetic surface at the outer plasma edge. It is consistent with the experimental observations that the frequency of ICE(T) is somewhat lower than the cyclotron frequency of T-ions as indicated in Fig.6(b). The slow Alfvén wave is well-known to be unstable due to the temperature anisotropy as in the case of AIC-modes. The slow wave branch can be unstable when the minority T-ions with the temperature anisotropy are included in the calculation. The anisotropy of T-ions at the outer plasma edge is evaluated in the next section.

4.2 Large Excursion Orbits

The orbits of FP-ions born in the plasma are calculated by using 'Escape Particle Orbit analysis Code (EPOC)'. In Fig.7, the orbits of ^{3}He and T-ions, which start inside the plasma and reach to the outer plasma edge, are indicated. It is shown that ^{3}He-ions from the center region cannot reach to the edge and T-ions from the center can reach to the edge region. The main source of FP-ions at the outer plasma is considered to be those born inside the plasma with large excursion orbits. As mentioned in the previous sub-section, the branch of the slow Alfvén wave will become unstable due to the anisotropy of T-ions. To evaluate the anisotropy of the energy distribution of T-ions at the plasma edge that come from the center region with such large excursion orbits, the pitch angle distribution of T-ions at the outer plasma edge is estimated by using EPOC. The anisotropy of T-ions deduced from the simple model for the pitch angle distribution and the deposition profile of N-NB becomes around 5. The experimental observation of ICE(T), of which frequency is much lower than the cyclotron frequency of T-ions at the outer plasma edge, is consistent with the excitation of slow Alfvén wave due to the anisotropy of the velocity distribution of T-ions.

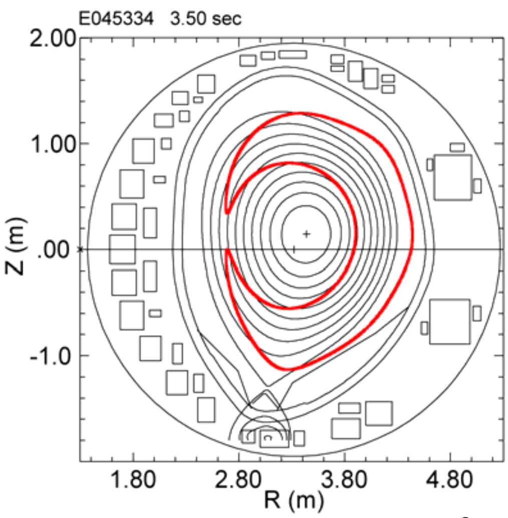

FIG.7(a) The large excursion orbit of ^{3}He-ions born near the central region which can reach the plasma edge.

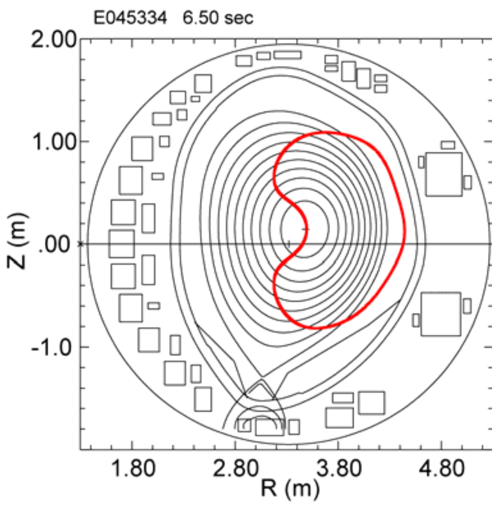

FIG.7(b) The large excursion orbit of T-ions born near the central region which can reach the plasma edge.

5. Summary

In this paper, ion cyclotron emissions (ICEs) due to deuterium-deuterium fusion-product ^{3}He, T and P-ions on JT-60U are described. The electromagnetic waves are measured by using ion cyclotron range of frequency antennas. The toroidal wave numbers are evaluated from the phase differences between two antenna straps arrayed in the toroidal direction. The excitation of the fast Alfvén waves (magneto-acoustic waves) for ICEs due to ^{3}He and P-ions, ICE(^{3}He) and ICE(P), is consistent with those in the previous JET and TFTR experiments. ICE(T) with lower frequency has larger wave numbers than ICE(^{3}He) in the same discharge. The excitation of slow Alfvén waves is elucidated for the first time as the mechanism for ICE due to T-ions, ICE(T). The density dependence of the excitation of ICE(^{3}He) is measured. The doublet peak of FP-ICEs due to two waves traveling in both toroidal directions is confirmed. The anisotropy of the FP T-ions at the outer plasma edge is evaluated by using 'Escape Particle Orbit analysis Code (EPOC)'. The precise behaviors of ICEs due to FP ions on JT-60U are studied.

Acknowledgments

The authors acknowledge the GAMMA 10 group at the University of Tsukuba and JT-60U team at Japan Atomic Energy Agency for their collaboration. This work is partly supported by Grant-in-Aid for Scientific Research under the Ministry of Education, Culture, Sports, Science and Technology, Japan (No.20026002) and also partly supported by the bidirectional collaborative research program of National Institute for Fusion Science, Japan (NIFS06KUGM014).

References

[1] Davidson, R.C., and Ogden, J.M., Phys. Fluids, **18** (1975) 1045.
[2] Smith, G. R., Casper, T. A., Gerver, M. J., Nuclear Fusion **23**, (1983) 1381.
[3] Ichimura, M., et al., Phys. Rev. Lett. **70** (1993) 2734.
[4] Cottrell, G.A., et al., Nuclear Fusion, **33** (1993) 1365.
[5] Dendy, R.O., et al., Phys. Plasmas **1** (1994) 1918.
[6] Cauffman, S. and Majeski, R., Rev. Sci. Instrum., **66** (1995) 817.
[7] Dendy, R.O., et al., Nuclear Fusion, **35** (1995) 1733.
[8] Kimura, H., et al., Nuclear Fusion, **38** (1998) 1303.
[9] Ichimura, M., et al., Nuclear Fusion, **48** (2008)035012.
[10] OYAMA, N. and JT-60 Team, Fusion Energy 2008, OV/1-3.
[11] Cauffman, S., et al., Nuclear Fusion, **35** (1995) 1597.